A LABORATORY STUDY: EXAMINING THE USE OF MINERAL FIBRE INSULATION TO ASSIST THE VENTILATION DRYING OF INTERNALLY INSULATED MASONRY WALLS

David Wach, Kim Pressnail, Ekaterina Tzekova

ABSTRACT

Providing a means of drying from the inboard face assists in the overall drying of the façade when masonry walls are insulated from the interior. To explore methods of improving the drying potential, two field studies were carried out on internally insulated historic masonry buildings in Toronto, Ontario. In these field studies, a vented drying airspace was created between the polyurethane foam insulation and the exterior solid masonry using a 12.5 mm polypropylene mesh. The polypropylene mesh was found to be an effective means of assisting drying of the masonry. However, to reduce construction costs, alternative systems were considered. One option investigated was using mineral fibre insulation to assist ventilation drying. Preliminary laboratory tests simulating inward vapour pressure drives induced by solar heating were carried out on an air-permeable mineral fibre insulation of various densities. Following these favourable preliminary tests, experimental procedures were modified in order to quantify the amount of drying that was occurring through the mineral fibre insulation. Multiple samples of RSI4.2 (R24) mineral fibre batts were tested with various airspace thicknesses. The testing revealed that the drying potential of mineral fibre insulation was roughly equivalent to a 3 mm (1/8 in.) vented clear airspace. Further, combining mineral fibre insulation with a 6 mm (1/4 in.) airspace was shown to be a very effective means of providing the ventilation necessary for drying solar heated walls. The laboratory test results were incorporated into a hygrothermal computer model to simulate the potential for drying walls exposed to moisture. Overall, the laboratory tests and the computer modeling have revealed that using air permeable insulation can be an effective means of assisting the drying of internally insulated walls.

BACKGROUND

In Canada, buildings account for roughly 30% of secondary energy use (Canadian Green Building Council, 2017). In the residential sector, approximately 2/3 of this energy is used for heating (Natural Resources Canada, 2015). Much of this energy use can be attributed to thermally inefficient older buildings. Thermally retrofitting older buildings that are still serviceable is a common energy-use reduction strategy. While it is often less expensive to insulate externally, internal insulation is often a necessity. For example, in the case of historic buildings, or buildings with lot restrictions, internal insulation is often the only viable strategy.

Internally insulated walls reduce the amount of heat transfer through the solid masonry structure during the heating season. This means that there is less energy available to dry moisture that has accumulated in the masonry wall. Thus, internally insulated walls are colder and damper. Cold and damp masonry walls may

be less durable. Durability issues include an increase in frequency of spalling due to osmotic pressures and freeze-thaw action. As well, wood floor joists or steel members that are embedded in the wetter masonry may fail since wood floor joists may decay and steel members may corrode in high relative humidity environments.

How durable masonry is depends on several factors, including the quality of the brick. Prior to advances in brick production in the mid-20th century, high variability in the mechanical properties of clay bricks existed, causing the properties of bricks used in solid brick masonry walls of historic buildings to be variable. During firing, temperature gradients in stationary kilns caused variations in the strength and absorption properties of clay bricks (Laefer et. al, 2004). Whether a brick will be susceptible to freeze-thaw damage depends on several factors, but a good measure of durability is the critical degree of saturation (S_{crit}) of the brick (Straube et al., 2010). In historical construction practice, common brick, with weaker mechanical properties, was often used for the inner wythes of solid masonry walls. This brick usually has a lower S_{crit} and is therefore more susceptible to freeze-thaw damage at a given moisture content. When a solid masonry wall is insulated internally, the interior wythes experience more freeze-thaw cycles. More vulnerable bricks that are more moist, and experience more freeze-thaw cycles are more likely to experience durability problems.

The risk of decay of embedded wooden floor joists also increases when masonry walls are internally insulated. Since the solid masonry walls are colder and wetter following internal insulation, the moisture content of the wood rises as the relative humidity of the air in contact with the wood rises (Guizzardi et al., 2015). The relative humidity threshold for decay to occur at building envelope surfaces is approximately 95% (Straube and Burnett, 2005).

De Rose et al. (2015) have investigated a limit state approach to evaluating the durability risk of insulating solid masonry walls in a cold climate. Risk from freeze-thaw, wood rot and corrosion is evaluated by comparing anticipated environmental loads (temperature and moisture) to loads levels that are necessary to damage the wall (De Rose et. al, 2015). Corrosion is measured by the time in which a metal is exposed to temperatures greater than 0°C and a relative humidity over 80% (Straube and Burnett, 2005). In the two case studies investigated by De Rose et. al, there was low freeze-thaw risk after the interior insulation retrofit due to the relatively high S_{crit} of the bricks, but the risk of wood rot and corrosion risk was increased.

To address these potential durability issues, ventilation drying should be considered. Past research has shown that ventilated airspaces included in wall assemblies with various types of cladding including brick masonry can promote drying (Straube and Finch, 2007). When a clear airspace is connected to exterior air through ventilation holes, convective forces within the clear airspace cause ventilation airflow which can remove moisture evaporating from materials in contact with air in the clear airspace. This strategy was investigated by researchers at The University of Toronto (Tzekova, 2015) in two field trials. In these field studies, a drying airspace was incorporated between polyurethane foam insulation and the masonry by using a polypropylene mesh that is commonly used to protect airspaces during brick veneer construction. The polypropylene mesh was found to be an effective means of assisting drying of the masonry because the ventilated airspace provided a secondary path for which the masonry could dry. The risk of freeze-thaw damage, steel member corrosion, and wood member decay was therefore reduced.

Since the polypropylene mesh is expensive, an alternate way of providing a vented airspace was sought. One option investigated by Tzekova (Tzekova and Pressnail, 2016) utilized air and vapour permeable mineral fibre insulation to assist ventilation drying. Preliminary laboratory tests simulating inward vapour pressure

drives generated by solar heating were carried out on air-permeable mineral fibre insulation of various densities. The results indicated that ventilation airflow did occur within the mineral fibre insulation and did promote drying. By utilizing mineral fibre insulation in a wall configuration to promote ventilation drying, both material and labour costs could be reduced. Further, additional thermal resistance could be provided compared to the polypropylene mesh approach. Thus, the use of mineral fibre insulation provided two functions: a thermal control function and a ventilation drying function.

LABORATORY TESTS

To quantify the effectiveness of mineral fibre insulation to function as a vented airspace, a series of laboratory tests were carried out. This section describes the laboratory testing. Multiple samples of RSI4.2 (R24) mineral fibre batts were tested with various airspace thicknesses. These laboratory tests continue the preliminary work performed by Tzekova at the University of Toronto.

Apparatus and Sample Preparation

Testing was performed in the climate simulator in the Building Science Laboratory at the University of Toronto. Figure 1 shows the layout of the climate simulator. The climate simulator was divided into two rooms, the Warm Room and the Cold Room. The Cold Room contained a chiller, and the set point of the room was -15°C. The temperature of the Warm Room was influenced by the temperature of the main laboratory which was approximately 21-23°C throughout testing. Two guard rooms, one within the warm room and one within the cold room, were constructed. The temperatures of the guard rooms were controlled by a combination of heaters and fans. The temperature of Guard Room 1 was maintained between 19-21°C and the temperature of Guard Room 2 was maintained between 18-21°C. The heaters and fans were controlled through relays by an HTBasic program. Data were collected from thermocouples and relative humidity sensors using an HP data acquisition unit.

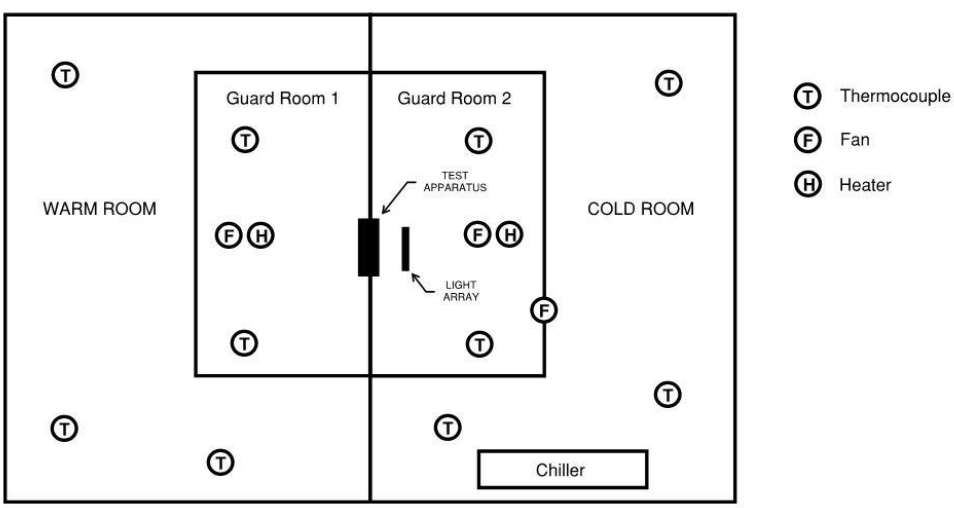

Figure 1: Plan View of Climate Simulator Set-up

To minimize evaporation losses during assembly and disassembly of the samples, the experimental apparatus

and procedures used by Tzekova were refined. Figure 2 shows a photograph of the test box apparatus, and Figure 3 shows a cross section of this apparatus which was used to measure moisture removal by ventilation. First, the test box cavity was loaded with RSI4.2 (R24) mineral fibre insulation which had been weighed. A tight fit at edges of the cavity was achieved when installing the mineral fibre insulation by using insulation with a width slightly larger than that of the cavity. Next, moist ship-lapped pine siding which acted as the moisture source was placed over the test cavity. Pine siding was chosen as a moisture source to allow for rapid apparatus construction. It is not intended to mimic the hygrothermal properties of masonry. The pine siding boards were moistened by immersing them in cold water for approximately 24 hours before the test. The pine boards were then removed from the water 30 minutes prior to installation to allow most of the surface moisture to evaporate. The pine boards were then weighed immediately prior to assembly. After the insulation was loaded into the test box cavity and the pine siding boards were installed, the apparatus was sealed. The gap between the moist siding and the mineral fibre insulation was maintained using wood spacers on the rails and stiles of the test box. The face and sides of the pine siding boards were then sealed with 0.15 mm polyethylene and construction tape. Any exposed wood was covered with construction tape to avoid moisture absorption. Circular ventilation holes were drilled into the pine boards at top and the bottom of the test apparatus. Corresponding holes were cut within the polyethylene sheet. A plastic grommet and tape were used to seal the circular vent hole ensuring that all airflow through the ventilation hole entered the test box cavity and did not leak between the boards and the polyethylene.

Figure 2: Photo of Test Box Apparatus

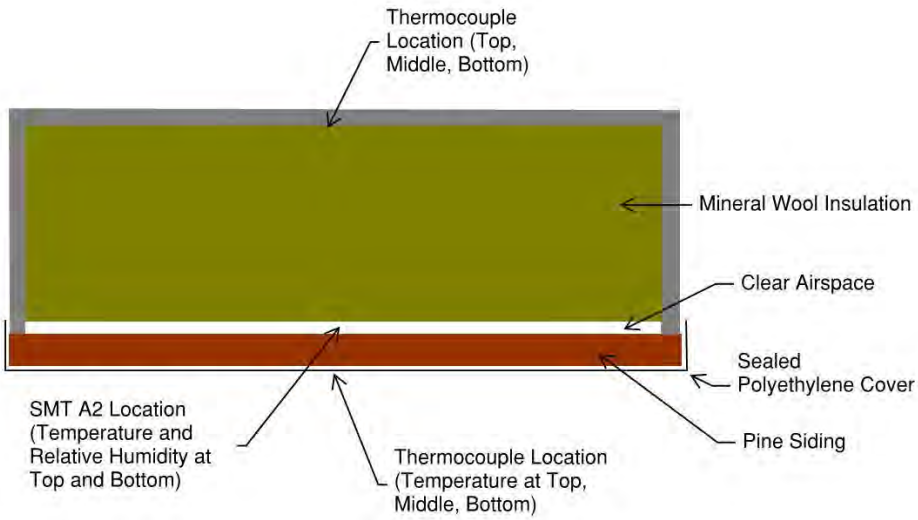

Figure 3: Cross Section of Test Apparatus

A light array increased the pine board temperatures creating a vapour pressure gradient to drive moisture from the pine boards into the test box cavity to simulate sun driven moisture from a cladding into a wall assembly. Six bulbs in a single column delivered approximately 1110 Watts to the polyethylene covered pine siding. Considering the total area of the pine boards, the average supplied power was 1288 W/m^2. The light array was positioned 30 cm away from the pine siding surface during testing. Thermocouples were installed at the top, middle and bottom at the back of the testing apparatus cavity. Thermocouples were also installed at the top, middle and bottom of the polyethylene to indirectly measure the surface temperature of the pine siding. SMT A2 wireless data loggers were used to record the temperature and relative humidity at the mineral fibre and pine siding interface (SMT, 2017). These sensors were positioned at the top and bottom of each wall, and were nested within cut-outs of the mineral fibre insulation.

Experimental Procedure

After the test box had been assembled with mineral fibre insulation and moist pine siding, and once it had been sealed, it was ready for testing. The assembled test box was mounted into the wall separating the two guard rooms and was exposed to the light array for 6 hours. The test apparatus was then disassembled and all the components were reweighed. A moisture mass balance was carried out to determine the quantity of moisture removed during the test.

In order to determine how much ventilation drying had occurred, it was necessary to do a mass accounting of the moisture. Difficulties arose in estimating the amount of moisture removed by ventilation because some of the moisture evaporated from the apparatus into the laboratory air during set up and disassembly. Further, surfaces including the polyethylene cover, the test box, and taped rails and stiles could not be readily weighed. So evaporation losses and losses on surfaces that could not be weighed became “unaccounted for moisture”. Finally, there was one more possible source of unaccounted for moisture. Although care was taken to ensure the testing apparatus was airtight, it is likely that some moisture may have been lost through unintentional air leakage. The quantity of moisture lost due to unintentional air leakage from the testing apparatus was also a source of unaccounted for moisture.

To estimate the quantity of the unaccounted for moisture, a base case test was set up. In the base case test,

the apparatus was completely air sealed using polyethylene sheeting. No ventilation holes were provided. This sample was then tested and the results revealed that the total quantity of moisture that was unaccounted for was approximately 10% of the total moisture supplied by the pine boards. Since the experimental procedures and sample preparations were the same for all tests, it was assumed that 10% of the moisture supplied was unaccounted for in all of the subsequent tests.

Once testing was completed, and the moisture accounting was carried out, two cases were considered. In the first case, it was assumed that none of the unaccounted for moisture was removed by ventilation. In the second case, it was assumed that all of the unaccounted for moisture was removed by ventilation. The former assumption likely leads to an underestimate of the amount of ventilation drying and is, therefore, a lower bound value. The latter assumption likely leads to an overestimate of the amount of ventilation drying and is an upper bound value. The actual amount of moisture removed by ventilation likely lies between the lower bound and the upper bound. In the analyses that follow, the average of the lower bound and the upper bound values was used to estimate the quantity of moisture removed by ventilation.

Results and Discussion

A series of tests were conducted using RSI4.2 mineral fibre batt insulation placed inside the test apparatus. Various vented space dimensions were tested including: 6 mm batt compression with no clear airspace (0 mm), no batt compression with no clear airspace (0 mm), 3 mm airspace, and 6 mm airspace. The quantity of moisture removed by ventilation was then determined for each configuration. Table 1 provides a summary of the tests performed and the resulting moisture supplied by the wood siding. As well, the resulting average vapour pressure difference, and the average stack pressure difference are also reported. During the tests summarized in Table 1, the vent area ratio was a constant 1175 mm^2/m^2. The vent area ratio is defined as ratio of the total vent area (mm^2) to the surface area of the wall tested (m^2).

Table 1: Testing Summary

Test Set	Test	Insulation Type	Clear Airspace Thickness (mm)	Vent Area Ratio (mm^2 / m^2)	Moisture Supplied by Wood Siding (g)	Vapour Pressure Difference (Pa)	Stack Pressure Difference (Pa)
8	8A	R24	6	1175	241	1040	1.84
	8B	R24	6	1175	282	1490	1.82
	8C	R24	6	1175	292	1870	2.09
9	9A	R24	0	1175	219	3180	1.94
	9B	R24	0	1175	215	3270	1.81
	9C	R24	0	1175	243	4090	2.44
11	11A	R24	0 (C)	1175	232	2640	1.82
	11B	R24	0 (C)	1175	252	3340	2.07
	11C	R24	0 (C)	1175	238	3300	2.00
13	13A	R24	3	1175	288	2809	2.05

	13B	R24	3	1175	281	1940	1.63
	13C	R24	3	1175	261	3370	2.30
	13D	R24	3	1175	276	1870	1.78

(C) denotes 6 mm compression of the batt

The quantity of moisture supplied during the 6 hour tests ranged from 215 g to 292 g. The average relative humidity in the Guard Room 2 was approximately 20% and the average relative humidity at the outboard surface of the batt was approximately 90%. Heating of the moist siding using the lamp array created a stack pressure difference between the bottom vent hole and the top vent hole. Based on the average temperature and relative humidity conditions, the average theoretical stack pressure difference was calculated for each test. This pressure difference varied between tests, but ranged between 1.63 Pa and 2.44 Pa for all of the tests.

Using the gravimetric moisture measurements, the average rate of moisture removal by ventilation during the 6 hour test period was determined for multiple samples of each air space configuration. Since the average stack pressure difference during testing varied slightly between samples, it was necessary to find a means of normalizing the results to facilitate comparisons. For the purpose of normalization, it was assumed that the flow was governed by the air space geometry and not the area of the vents. Preliminary test results revealed that even at vent area ratios higher than 1175 mm^2/m^2, ventilation flow did not increase appreciably (Wach, 2017). This finding is consistent with flow in the airspace being determinative of the total flow. Studies by others including Straube and Burnett have shown that ventilation flow within air spaces can be assumed to be laminar (Straube and Burnett, 2005). Since laminar flow corresponds to a flow exponent of 1.0 then ventilation flow is directly proportional to the stack pressure difference. Thus, the existence of this direct relationship means that the flow results can be normalized by dividing the average rate of moisture removal by the average stack pressure difference. This latter step allowed the data to be compared on a per Pascal pressure difference. A summary plot of the average normalized rate of moisture removed by ventilation for each sample is shown in Figure 4.

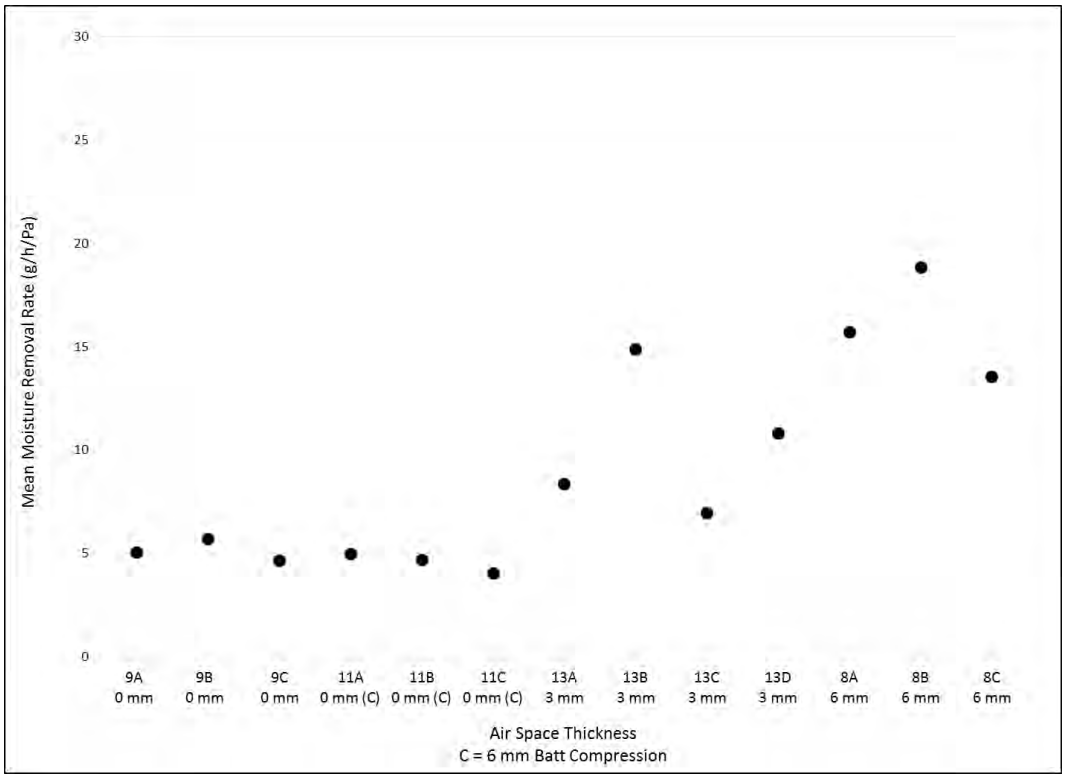

Figure 4: The Average Normalized Moisture Removal Rate for Various Air Space Thicknesses

Test Sets 9 and 11 both featured a venting configuration that included no clear airspace between the pine siding boards and the mineral fibre insulation. The insulation batts used in Test Set 11 were compressed by 6 mm to ensure more complete contact with the pine siding. In Test Set 9, the rate of moisture removed by ventilation per Pascal pressure difference ranged from 4.7 to 5.7 g/h/Pa. In Test Set 11 where the batts were compressed slightly, the rate of moisture removal ranged from 4.0-5.0 g/h/Pa. The normalized rate of moisture removal by ventilation during testing was slightly lower when the batts were compressed. The observed difference in the natural ventilation rate when the batts were compressed versus no compression may be within experimental error. However, when the batts are compressed, two effects occur. First, compression causes the local density of the batts to increase slightly, particularly at the interface with pine siding. This increase in density may lead to a slight increase in the resistance to air flow through the batts. Secondly, since the surface of the batt is not a plane surface, small interconnected void spaces likely exist between the surface of the batt insulation and the pine siding. When the batt is compressed, interconnected void spaces are less likely to occur and therefore fewer channels for airflow would exist.

In both Test Set 9 and Test Set 11 where no clear airspace was provided, moisture was still removed by ventilation. The results lead to the conclusion that some moisture can be removed by ventilation airflow within the mineral fibre insulation due to small pressure differences.

Test Sets 8 and 13 introduced a clear airspace to act in conjunction with any venting that was occurring through the mineral fibre insulation. A consistent thickness of the airspace during testing was achieved by adding wood spacers around the perimeter of the test apparatus. The clear airspace was located between the pine siding boards and the mineral fibre batts. By using 3 mm and 6 mm strapping, consistent air spaces were created.

Three samples were tested in the Test Set 8 series and featured a 6 mm airspace and mineral fibre batts. The

normalized rate of moisture removal ranged from 13.5-18.9 g/h/Pa. Adding a 6 mm clear airspace to the venting configuration increased the amount of moisture removed by venting compared to when no clear airspace was provided. Test Set 13 series involved four samples and featured a 3 mm airspace in the venting configuration. The normalized rate of moisture removal ranged from 7.0-14.9 g/h/Pa. Adding a 3 mm clear airspace increased the amount of moisture removed by venting as compared to when no clear airspace was provided in the venting configuration. As expected, the amount of moisture removed with a 3 mm air space was less than when a 6 mm air space was tested.

Figure 4 shows the mean normalized moisture removal rate for each air space thickness. The average rate of moisture removal for the 0 mm air space was 4.6 g/h/Pa with batt compression, and 5.1 g/h/Pa with no compression. The mean normalized rate of moisture removal was 10.3 g/h/Pa for the 3 mm tests and 16.0 g/h/Pa for the 6 mm tests.

The average rate of venting through the mineral fibre insulation with no clear air space was of 4.9 g/h/Pa. This rate was used as a baseline rate as shown in Figure 5. Using this baseline, and considering the 3 mm air space tests, it is likely that up to 4.9 g/h/Pa of the total 10.3 g/h/Pa of venting occurred through the batt insulation, and the remainder occurred through the air space. It can be inferred that venting through the RSI4.2 (R24) mineral fibre insulation is in the order of the venting through a 3 mm clear air space with air impermeable boundaries.

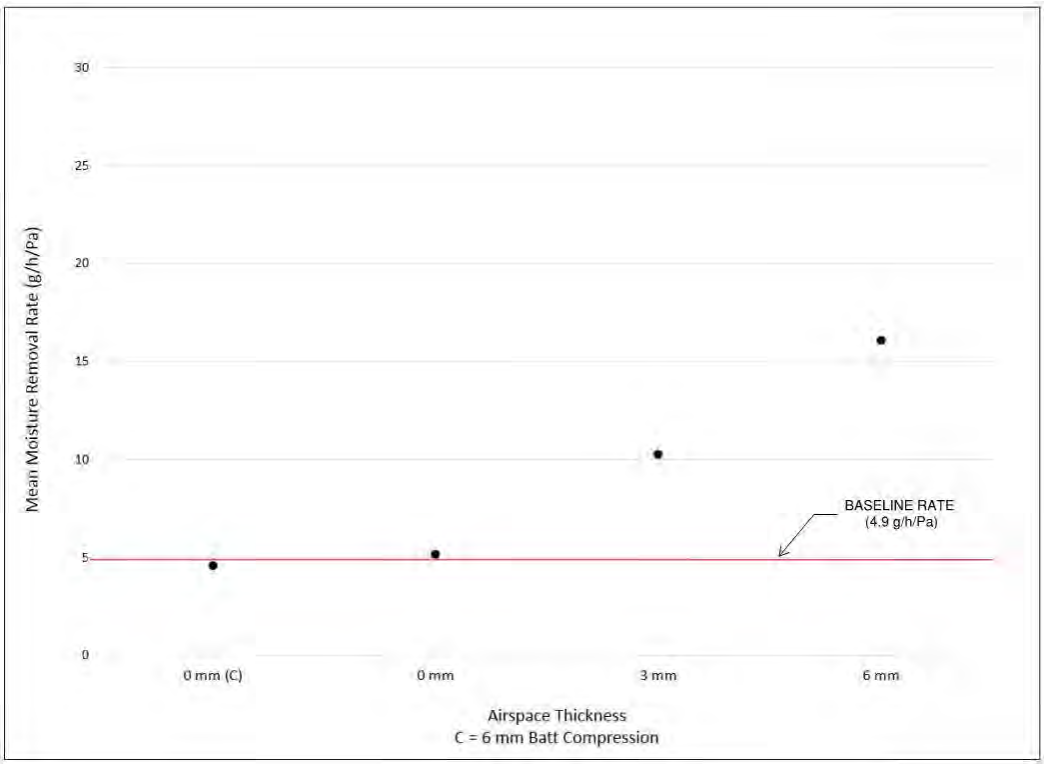

Figure 5: Average Normalized Moisture Removal Rate - Mean of Set at Airspace Thickness

If the same baseline is applied to the 6 mm air space samples, then we find that approximately 11.1 g/h/Pa of ventilation drying occurred within the clear air space. Given that the flow in the air space was likely laminar, not surprisingly, the flow in the air space roughly doubled when the thickness of the air space was doubled from 3 mm to 6 mm.

This leads to the question, was there any other evidence of ventilation drying occurring through the batt insulation? Further evidence that venting was occurring through the batt insulation can be found by examining the moisture content distribution within the batt insulation following each test. To facilitate gravimetric measurements, the batt insulation contained 5 different pieces of insulation stacked upon each other. As shown in Figure 6, more moisture was found in the upper most batt than in the lower most batt. This moisture distribution is consistent with air rising and passing through the insulation by convection. As the air was warmed it rose, and it gained moisture from the pine siding. Despite the warming of the air, eventually the air in the insulation reached its dew point and condensed within cooler areas of the batt insulation. This explanation is consistent with the higher moisture contents found in the upper most batt compared to the lowest batt.

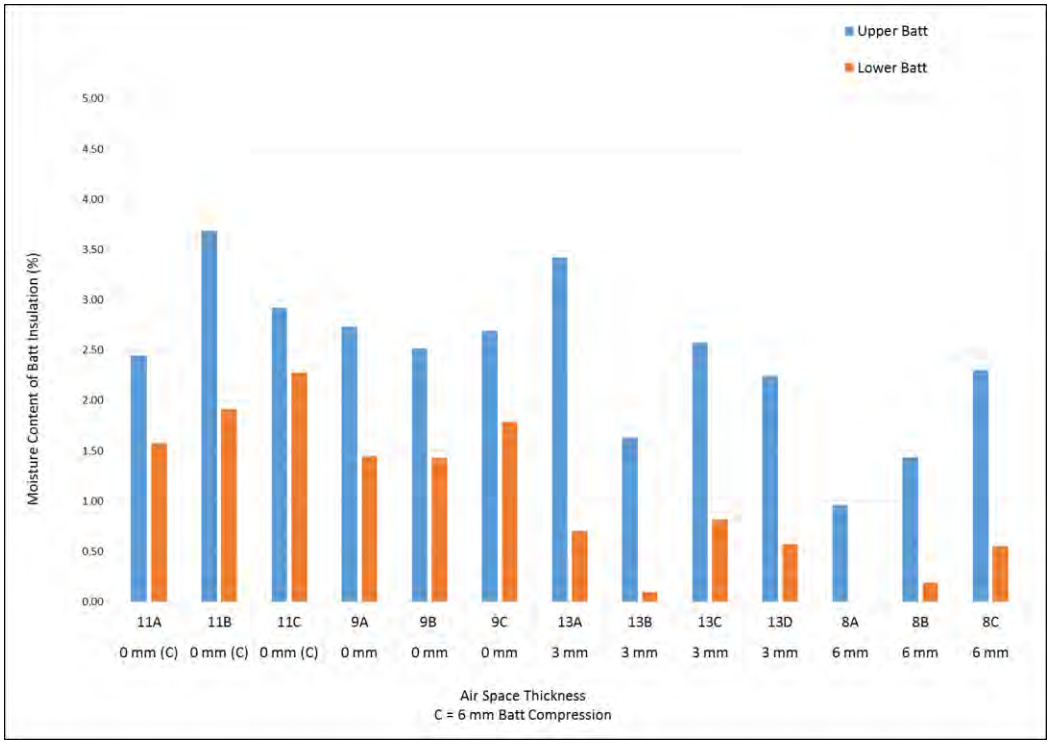

Figure 6: Moisture Content of Batt Insulation as a Percentage

Overall, the results of the laboratory testing suggest that airflow is occurring in the mineral fibre insulation. Moisture is being removed by ventilation even when no clear airspace is provided. As well, the vertical distribution of moisture within the insulation that was found upon test completion provides further evidence that convective airflow is transporting moisture within the insulation.

HYGROTHERMAL MODELING

The laboratory testing presented above has shown that ventilation drying can be achieved through mineral fibre insulation when moist façades which have been internally insulated are solar heated. The amount of venting that appears to be occurring through the insulation is in the order of venting through a clear airspace with a thickness of up to 3 mm. Considering this finding, hygrothermal model simulations were carried out using WUFI Pro 6 modeling software to investigate the potential impact of the ventilation drying on the response of an internally insulated wall system over a five year simulation period. Brick masonry was chosen

to illustrate the possible assistance that air permeable mineral fibre insulation can provide to the back-drying of moist façades.

In total, four venting conditions were simulated. The first case, was an internally insulated wall with no provision for ventilation drying. This case was labelled "No Venting," and models the case where no provisions have been made for back venting of the façade. The second case was a 3 mm air space which was used to simulate the venting that could occur in mineral fibre insulation with no clear air space. This step was necessary since the modelling program could not simulate flow through the mineral fibre insulation. Thus, a 3 mm air space was modelled in order to evaluate the potential effects of ventilation drying though the mineral fibre insulation with no clear air space. The third and fourth cases were 6 mm and 9 mm air spaces which were used to simulate the venting that could occur in mineral fibre insulation plus a 3 mm and a 6 mm clear air space respectively.

Model Set-Up

Simulations were carried out over a five-year time-period on the south and east orientations of a low-rise building located in Toronto, Ontario. These orientations were chosen because of they are most often exposed to driving rain. The simulations were carried out to determine if the wall assemblies were accumulating moisture over time or if they could dry out. Interior conditions were based upon operating conditions during testing at the Gemini building in Toronto (Tzekova, 2015), which had incorporated ventilated cavities behind solid masonry walls. Ventilation always occurred to the exterior during the simulations.

Table 2: WUFI Common Model Parameters

Model Parameter	Input
Rain Exposure	ASHRAE 160
Initial Material RH	80% (default WUFI value)
Simulation Runtime	5 years
Simulation Time Step	1 hour
Interior Boundary Conditions	23°C (1°C amplitude) 39% RH (15% amplitude)
Exterior Boundary Conditions	Toronto Cold Weather Year

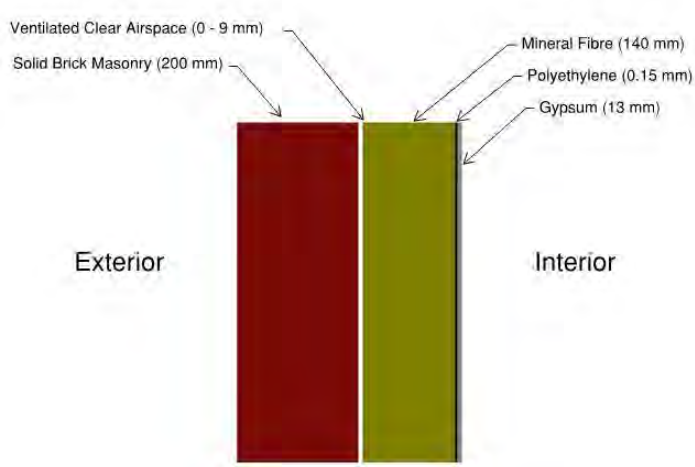

Figure 7: Wall Assembly for WUFI Simulations

Brick (old) was chosen because it had similar material properties to solid masonry bricks tested in Toronto

(Tzekova, 2015). Roxul ComfortBatt R-24 was chosen because it had been tested in the laboratory study reported here. In walls with a clear air space, the air layer was chosen to have no additional moisture capacity.

Table 3: Materials Used in Model

Material	WUFI Material	Database
Solid Masonry	Brick (old) (3 wythe equivalent)	North American
Mineral Fibre	Roxul ComfortBatt	ASHRAE 160
Ventilated Airspace	Air Layer 10mm	Generic Materials
Polyethylene	PE-Membrane (Poly;0.07 perm)	Generic Materials
Interior Gypsum	Gypsum Board (USA)	Fraunhofer-IBP

Constant ventilation rates through the clear air space were simulated for each of the venting configurations in which a clear air space was included. 10 ACH, 50 ACH and 100 ACH were simulated. These ventilation rates were chosen because similar rates had been observed behind solid masonry construction and reported for the Barrymore and Gemini field trials in Toronto, Ontario. At Barrymore, the reported averages were 30 ACH at the east face and 50 ACH at the south face (Tzekova, 2015). Average ventilation rates recorded at the Gemini House were approximately 100 ACH at both the north and south elevations (Tzekova, 2015).

Simulation Results and Discussion

The resulting average moisture content in the brick masonry during the five-year simulation period is shown in Figure 8 for each simulation at the south and east orientations. For both orientations, walls with ventilated air spaces have a lower average moisture content in the brick masonry when compared to those with no ventilation. In addition, as expected, the average moisture content of the brick masonry decreases as the ventilation rate increases for a given air space thickness.

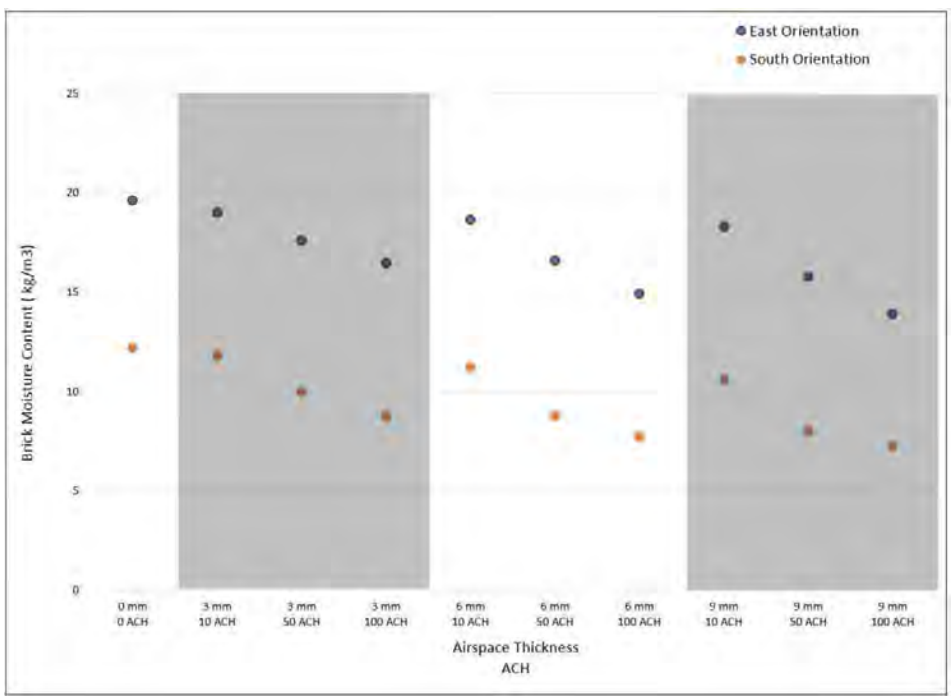

Figure 8: Average Moisture Content in Brick Masonry for Various Air Space Thicknesses and Air Change Rates

The wall assembly simulations with a 3 mm clear air space and 100 ACH ventilation rate has a lower average moisture content in its brick masonry than does wall modeled with a 9 mm airspace at 10 ACH at both elevations. When the ventilation rate in the wall with the 9 mm air space is increased to 100 ACH, the average

moisture content of the brick masonry is reduced to 7.3 kg/m^3 for the south elevation and 13.9 kg/m^3 for the east elevation. Given the airspace thicknesses and ventilation rates simulated, varying the ventilation rate has a larger impact than does varying the airspace thickness. With a ventilation rate of 100 ACH, a significant amount of drying is achieved in the brick masonry when a 3 mm air space is incorporated into the wall assembly, for walls in the south and east orientations.

Relative humidity at the exterior face of the mineral fibre insulation for various venting configurations at the ventilation rate of 100 ACH was also simulated. This location represents the interface between brick masonry and mineral fibre insulation when no clear air space is incorporated into the wall assembly. The location represents the interface between the ventilated air space and the mineral fibre insulation when a clear air space is present. The relative humidity at this location was in excess of 95% in the wall assembly when no ventilated air space was present during the majority of time in the simulation, at both orientations. By contrast, the relative humidity is lower for wall assemblies with a ventilated air space at the exterior portion of the mineral fibre insulation over the simulation period, at both orientations. Figure 9 shows the monthly average relative humidity over the simulation at the south orientation for each airspace thickness at 100 ACH.

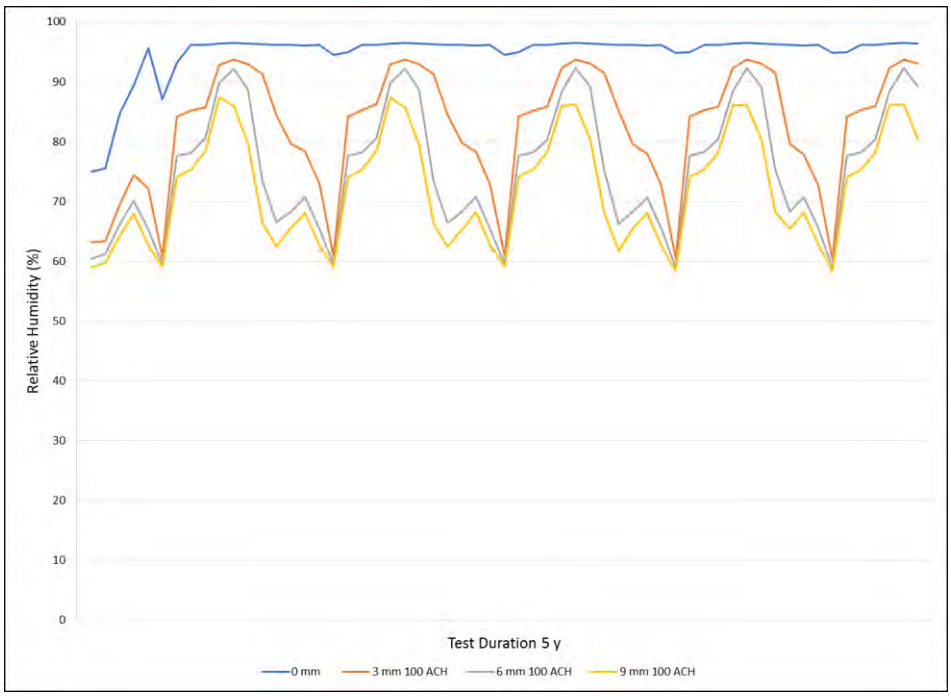

Figure 9: South Orientation: Relative Humidity at Outboard Edge of Mineral Fibre Insulation

Overall, the simulations have demonstrated the potential for incorporating ventilated air spaces behind solid masonry walls in Toronto, Ontario. The simulations have shown that introducing a ventilated air space into the wall assembly reduces the average moisture content of brick masonry and reduces the relative humidity in walls in the south and east orientations. The average moisture content and relative humidity in the wall assembly is lower at the south face than it is at the east face. The east face experiences more driving rain events in the simulated climate and has less solar exposure.

The amount of drying in the wall assemblies increases as the air space thickness increases and as the ventilation rate is increased. The simulations have shown that a vented air space as small as 3 mm can reduce the average moisture content and the relative humidity in the wall assembly. This reduces the potential for freeze-thaw damage to susceptible brick, and rot and corrosion of embedded structural members.

The 6 mm venting configuration in the model may be most representative of a venting configuration incorporating mineral fibre insulation. If mineral fibre venting is assumed to be in the order of venting provided by a 3 mm airspace, then the addition of a 3 mm clear air space to the mineral fibre insulation provides significant drying. If the mineral fibre insulation is not compressed against the inside face of the masonry when it is installed, voids due to the interior roughness of the brick masonry can add additional thickness to the ventilated air space.

The simulations reveal the drying benefits of ventilation. The amount of drying increases significantly as the ventilation rate is increased. There was a relatively small reduction in average moisture content when a ventilation rate of 10 ACH was simulated with the different clear air space thicknesses. The most benefit was shown when 100 ACH was simulated. The average ventilation rate falling in the range 50 to 100 ACH is a reasonable assumption for the south and east faces based upon field data previously obtained in Toronto. Rates may be lower at the north face, due to less exposure to solar radiation that drives some of the ventilation airflow, although wind would still be acting to assist in ventilating a north façade.

There are several limitations to the simulations. The materials used were chosen from generic databases. The properties of materials in existing buildings in Toronto may not be represented. Properties will vary from building to building, even in the same geographic location. Another significant limitation is choosing a constant rate of ventilation for the simulations. The ventilation rate would change significantly over both the short term and the long term. The ventilation rate is a function of both building characteristics and environmental factors and would not be the same across buildings located in Toronto. A constant ventilation rate gives us an indication on average of the moisture that can be removed by ventilation behind solid masonry in a wall assembly.

CONCLUSIONS

The laboratory tests examined the potential for mineral fibre insulation to act as a venting medium in wall assemblies. The results of the laboratory experiments reveal that ventilation drying can occur through air permeable mineral fibre insulation if appropriate vents are provided. When combined with a vent area ratio of 1175 mm^2/m^2, the drying that occurs through RSI4.2 mineral fibre insulation is roughly equivalent to a 3 mm clear air space. Further, testing showed that using a combination of mineral fibre insulation with a clear air space increases the amount of moisture that can be removed by ventilation. However, this testing occurred with a vent area ratio of 1175 mm^2/m^2. Further testing of a range of vent area ratios will assist in determining the optimum vent area ratio.

The model simulations revealed that in a drying climate like Toronto ON, introducing ventilation into solid masonry wall assemblies reduces the average moisture content and relative humidity of the solid masonry walls. Ventilation drying through even relatively small air spaces or even through air permeable insulation, improves the drying potential.

Improving the drying potential of solid masonry walls that have been internally thermally retrofitted in heating climates means that embedded wood members will be less likely to decay and steel members less likely to corrode. Further, the masonry will be less likely to reach its critical saturation point, reducing the freeze-thaw risk to susceptible brick as walls become colder when internal insulation is added. To reduce risk when internally insulating, designers should consider the durability of wall components when specifying

retrofit insulations. Using mineral fibre insulation coupled with appropriate vents can improve the durability of internally insulated solid masonry walls.

ACKNOWLEDGEMENTS

The authors gratefully acknowledge support provided by the Natural Sciences and Engineering Research Council and Engineering Link Inc. The authors also acknowledge Roxul Inc. for their technical support for the laboratory testing.

REFERENCES

Canadian Green Building Council. 2017. Why green building. Available from http://www.cagbctoronto.org/cagbc-toronto/about-us [accessed 3 June 2017].

De Rose, D., Pearson, N., Mensinga, P., and Straube, J.F. 2015. Towards a Limit States Approach to Insulating Solid Masonry Walls in a Cold Climate. In Proceedings of 14th Canadian Conference on Building Science and Technology, Toronto, Ontario, 28-31 October, 2014. Available from http://obec.on.ca/CCBST2014/NEWS/index.php.

Guizzardi, M., Carmeliet, J., and Derome, D. 2015. Risk analysis of biodeterioration of wooden beams embedded in internally insulated masonry walls. Construction and Building Materials. **99**: 159-168.

Finch, G. and Straube, J. 2009. Ventilated Wall Claddings: Review, Field Performance, and Hygrothermal Modeling. Research Report 0907. Available from https://buildingscience.com/documents/reports/rr-0907-ventilated-wall-claddings-review-performance-modeling/view

Laefer, D., Boggs, J., Cooper, N. 2004. Engineering properties of historic brick: variability considerations as a function of stationary vs. non-stationary kiln types. Journal of the American Institute for Conservation. **43**(3):255-272.

Natural Resources Canada. 2015. Comprehensive Energy Use Database Table Residential Sector Canada. Available from http://oee.nrcan.gc.ca/corporate/statistics/neud/dpa/showTable.cfm?type=CP&sector=res&juris=ca&rn=2&page=0 [accessed 3 June 2017].

SMT, 2017, SMT Wireless Data Acquisition Unit. Available from http://smtresearch.ca/sites/default/files/resource/RS-1100%20SMT-A2%20Datasheet%20Web 0.pdf [accessed 20 November 2015].

Straube, J. and Burnett, E. 2005. Building Science for Building Enclosures. Building Science Press, Somerville, MA.

Straube, J., Schumacher, C., and Mensinga, P. 2010. Assessing the Freeze-Thaw Resistance of Clay Brick for Interior Insulation Retrofit Projects. In Proceedings of Buildings XI ASHRAE Conference, Clearwater Beach, Florida, 5-9 December, 2010. Available from

https://buildingscience.com/documents/confpapers/cp-1013-freeze-thaw-resistance-clay-brick-interior-insulation-retrofits/view

Tzekova, E.S. 2015. Improving the thermal performance and durability of historic masonry buildings. PhD. Thesis, Department of Civil Engineering, University of Toronto, Toronto, ON.

Tzekova, E.S., Pressnail, K.D. 2016. Using Fibre Insulation as a Means of Drying Internally Insulated Walls. In Proceedings of Buildings XIII ASHRAE Conference, Clearwater Beach, Florida, 4-8 December, 2016.

Wach, D.R. 2017. Improving the Durability of Thermally Insulated Historic Solid Masonry Walls. MASc. Thesis, Department of Civil Engineering, University of Toronto, Toronto, ON.